





Article

CDC20 Is Regulated by the Histone Methyltransferase, KMT5A, in Castration-Resistant Prostate Cancer

Zainab A. H. Alebady ^{1,2}, Mahsa Azizyan ¹ , Sirintra Nakjang ³, Emma Lishman-Walker ¹, Dhuha Al-Kharaif ⁴, Scott Walker ⁵, Hui Xian Choo ¹, Rebecca Garnham ¹, Emma Scott ¹ , Katya L. Johnson ¹, Craig N. Robson ⁶  and Kelly Coffey ^{1,*} 

¹ Biosciences Institute, Newcastle Cancer Centre, Newcastle University, Newcastle upon Tyne NE2 4HH, UK

² Department of Laboratory and Clinical Science, College of Pharmacy, University of AL-Qadisiyah, Al-Diwaniya 58002, Iraq

³ Bioinformatics Support Unit, Newcastle University, Newcastle NE2 4HH, UK

⁴ Medical Laboratory Technology Department, College of Health Sciences, Public Authority of Applied Education and Training, Safat 13092, Kuwait

⁵ School of Medicine, Newcastle University, Newcastle upon Tyne NE2 4HH, UK

⁶ Translational and Clinical Research Institute, Newcastle Cancer Centre, Newcastle University, Newcastle upon Tyne NE2 4HH, UK

* Correspondence: kelly.coffey@newcastle.ac.uk

Simple Summary: The methyltransferase KMT5A is suggested as an oncogene in prostate cancer but the mechanisms underlying its oncogenic properties are poorly understood. This study uncovers genes and cellular pathways which are regulated by KMT5A in prostate cancer to obtain a better understanding of whether or not therapeutic targeting is viable. In particular, we focus on the key cell cycle protein, CDC20, which we reveal to be a KMT5A-regulated gene via two mechanisms; 1. the methylation of histone H4K20 within the *CDC20* promoter to enhance *CDC20* transcription and 2. the inhibition of p53 via direct methylation to release *CDC20* transcriptional repression. Furthermore, we demonstrate that *KMT5A* and *CDC20* are positively correlated in clinical samples of prostate cancer. Due to the roles that *KMT5A* and *CDC20* play in cell cycle regulation and DNA repair processes, we propose that targeting the methylation activity of *KMT5A* will provide therapeutic benefits where these two oncogenic proteins are overexpressed.



Citation: Alebady, Z.A.H.; Azizyan, M.; Nakjang, S.; Lishman-Walker, E.; Al-Kharaif, D.; Walker, S.; Choo, H.X.; Garnham, R.; Scott, E.; Johnson, K.L.; et al. CDC20 Is Regulated by the Histone Methyltransferase, KMT5A, in Castration-Resistant Prostate Cancer. *Cancers* **2023**, *15*, 3597. <https://doi.org/10.3390/cancers15143597>

Academic Editors: Trever G. Bivona and Wei Wu

Received: 26 May 2023

Revised: 6 July 2023

Accepted: 11 July 2023

Published: 13 July 2023



Copyright: © 2023 by the authors. Licensee MDPI, Basel, Switzerland. This article is an open access article distributed under the terms and conditions of the Creative Commons Attribution (CC BY) license (<https://creativecommons.org/licenses/by/4.0/>).

Abstract: The methyltransferase KMT5A has been proposed as an oncogene in prostate cancer and therefore represents a putative therapeutic target. To confirm this hypothesis, we have performed a microarray study on a prostate cancer cell line model of androgen independence following KMT5A knockdown in the presence of the transcriptionally active androgen receptor (AR) to understand which genes and cellular processes are regulated by KMT5A in the presence of an active AR. We observed that 301 genes were down-regulated whilst 408 were up-regulated when KMT5A expression was reduced. KEGG pathway and gene ontology analysis revealed that apoptosis and DNA damage signalling were up-regulated in response to KMT5A knockdown whilst protein folding and RNA splicing were down-regulated. Under these conditions, the top non-AR regulated gene was found to be *CDC20*, a key regulator of the spindle assembly checkpoint with an oncogenic role in several cancer types. Further investigation revealed that KMT5A regulates *CDC20* in a methyltransferase-dependent manner to modulate histone H4K20 methylation within its promoter region and indirectly via the p53 signalling pathway. A positive correlation between KMT5A and *CDC20* expression was also observed in clinical prostate cancer samples, further supporting this association. Therefore, we conclude that KMT5A is a valid therapeutic target for the treatment of prostate cancer and *CDC20* could potentially be utilised as a biomarker for effective therapeutic targeting.

Keywords: CDC20; biomarker; KMT5A; p53; prostate cancer

1. Introduction

Prostate cancer is the most common cancer in men in the UK. Whilst androgen receptor (AR)-targeting therapies have yielded significant patient benefits, relapse to treatment is a significant clinical problem. Hence, there is an urgent need to develop alternative therapeutics to treat advanced disease. The lysine methyltransferase, KMT5A, plays an oncogenic role in a number of cancers [1–3]. Indeed, KMT5A siRNA-mediated knockdown inhibits prostate cancer cell proliferation and KMT5A has been identified as an AR-interacting protein that is required for the transcription of the AR-regulated gene, *prostate specific-antigen* (PSA), via the promotion of mono-methylation on histone H4 at lysine 20 (H4K20Me1) at the PSA promoter [4]. Furthermore, KMT5A plays a role in the epithelial–mesenchymal transition (EMT) and enhances the invasiveness of prostate cancer cell line models, independent of the AR through its interplay with ZEB1 [5]. Initially identified as the sole methyltransferase responsible for H4K20Me1, KMT5A was subsequently shown to methylate numerous other non-histone proteins, including p53 [6]. A greater understanding of KMT5A in the context of prostate cancer is required to determine whether or not it is a bona fide therapeutic target.

KMT5A activity is regulated via post-translational mechanisms during specific phases of the cell cycle. During the late S phase and at the G2/M transition, the levels of KMT5A are at their peak and found localised to mitotic chromosomes. As the cell moves through prophase to anaphase, KMT5A is phosphorylated at serine 29 by cdk1/cyclin B. This results in KMT5A dissociation from chromatin and stabilisation via the inhibition of KMT5A association with the APC^{cdh1} E3 ubiquitin ligase [7]. During anaphase, KMT5A is dephosphorylated by cdc14a/b, which in turn permits protein turnover to reduce KMT5A protein levels at G1. During G1, KMT5A levels are sustained, however, during the G1/S transition, SCF^{skp2} ubiquitin ligase targets KMT5A for protein turnover resulting in undetectable KMT5A protein. Interestingly, KMT5A interacts with the proliferating cell nuclear antigen (PCNA) at DNA replication foci and is essential for correct DNA replication [8] suggesting a high turnover rate of chromatin bound KMT5A by CRL4^{cdt2} [7]. The alterations in the levels of KMT5A throughout the cell cycle are mirrored by H4K20Me1 levels suggesting that methyltransferase activity is predominantly regulated by cellular KMT5A levels.

Cell cycle division 20 homologue (CDC20) is a cell cycle regulatory protein implicated in the spindle assembly checkpoint (SAC) and is required for cells to progress through mitosis. Specifically, CDC20 functions as a substrate recognition molecule and activator of APC to result in the ubiquitin-mediated turnover of its substrates. In particular, APC^{CDC20} functions during metaphase to anaphase to result in the destruction of cyclin B and securin, thereby allowing sister chromatids to segregate. CDC20 activity is inhibited by the mitotic checkpoint complex (MCC) and is only released to target its substrates once microtubule binding to the kinetochore and appropriate tension is achieved, thereby preventing genomic instability. Interestingly, there are suggestions that CDC20 may play a role in the DNA damage repair pathway via RAP80 [9] and REV1 [10] down-regulation. Furthermore, DNA damage-induced p53 can directly inhibit the expression of CDC20 by associating with the CDC20 promoter region and causing chromatin remodelling [11]. In addition, p21 can inhibit CDC20 mRNA by associating with CDE-CHR elements in the CDC20 promoter [12]. The depletion of PHF8, an H4K20Me1 demethylase, results in prolonged G2 and defective mitosis and it is itself a substrate of APC^{CDC20} [13] further suggesting that chromatin remodelling can be influenced by CDC20 levels.

CDC20 has been proposed to exhibit an oncogenic role in a number of cancers including prostate cancer [14]. Indeed, biochemical recurrence-free survival is lower in patients with high levels of CDC20 compared to patients with low CDC20 expression [15]. CDC20 itself is a target for ubiquitination by the E3 ligase SPOP, which is commonly mutated and non-functional in prostate cancers, providing an explanation for elevated CDC20 levels [16]. Furthermore, CDC20 expression is associated with resistance to docetaxel [16,17] and is implicated in the wnt/Beta-catenin pathway which is oncogenic in advanced prostate cancer [17,18].

The aim of this study was two-fold; the first aim was to use pathway analysis to provide further evidence that KMT5A regulates oncogenic pathways and is a valid therapeutic target in prostate cancer and the second was to identify individual genes that are regulated by KMT5A in a model of castration-resistant prostate cancer as potential biomarkers for KMT5A activity. Indeed, we show that a number of oncogenic pathways are down-regulated upon KMT5A knockdown and we identified and validated CDC20 as a KMT5A-regulated gene.

2. Materials and Methods

2.1. Antibodies

Antibodies used in this study included KMT5A (cell signalling), CDC20 (Ab190711, and AbCam), PARP1/2 (clone H250, sc-7150, Santa Cruz Biotechnology, Dallas, TX, USA), MDM2 (Clone N-20, sc-813, Santa Cruz Biotechnology), p21 (ab-4, Calbiochem), p53 (pAb-421#OP03, Calbiochem), p53-S15-P (cell signalling), p53-K382-Ac (ab75754, AbCam), H4K20Me1 (Ab9051, AbCam), H4 (07-108, Merck, Darmstadt, Germany), anti-phosphohistone H2AX (Ser139) (clone JBW301, Millipore Corp., Burlington, MA, USA) α -tubulin (clone DM1A, T9026, Sigma, St. Louis, MO, USA), and GAPDH (clone 1E6D9, Proteintech, Rosemont, IL, USA).

2.2. Compounds

Dihydrotestosterone (DHT) (Sigma) was prepared in ethanol at a final concentration of 10 mM and stored at -80°C . KMT5A inhibitors UNC0379 (S7570, Selleckchem, Houston, TX, USA) and Ryuvidine (2609, R&D Systems, Minneapolis, MN, USA) were purchased in powder form and resuspended in DMSO to a final concentration of 50 mM and 20 mM, respectively. Solutions were stored at -80°C for no longer than 1 month. Nutlin 3 was provided by Prof. John Lunec (Newcastle Cancer Centre).

2.3. Cell Culture

LNCaP cells, a model of androgen dependence, and AR negative PC3 cells were purchased from American Type Culture Collection (Manassas, VA, USA); LNCaP-AI cells, a model of androgen independence, were generated in-house as described previously [19]. Cells were maintained as previously described [20].

Short tandem repeat profiling was used to authenticate the cell lines used in this study (NewGene, Newcastle upon Tyne, UK). MycoAlert (Lonza, UK) was used to routinely test for the presence of mycoplasma.

2.4. siRNA

The reverse transfection of cell lines with siRNA sequences (25 nM) was carried out using Lipofectamine RNAiMAX (Invitrogen) in accordance with the manufacturer's protocol. Either qPCR or Western blotting confirmed successful knockdown. Non-silencing (N/S): UUCUCCGAACGUGUCACGU[dT][dT]; siKMT5A_1: CCAUGAAGUCCGAG-GAACA[dT][dT]; siKMT5A_2: GATGCAACTAGAGAGACA[dT][dT]; siCDC20_1 CG-GAAGACCUGCCGUUACA[dT][dT]; siCDC20_2: GGGCCGAACUCCUGGCAAA[dT][dT].

2.5. Western Blotting and Quantitative Polymerase Chain Reaction

Western [21] and qPCR analysis [20] were performed as described previously. Primer sequences are detailed in Supplementary Table S1.

2.6. Microarray

Cellular RNA was extracted using Trizol[®] (Invitrogen, Waltham, MA, USA) and quality-checked using Agilent Bioanalyzer 2100 prior to analysis using Illumina HT-12 v4.0 Expression BeadChip (Oxford Genomics Centre, The Wellcome Trust Centre for Human Genetics, University of Oxford, Oxford, UK).

R package ‘Lumi’ was used for array processing, background correction, normalisation and quality control checks. Variance-stabilising transformation was used to convert probe intensity values to VSD (variance-stabilised data). The array normalisation method used was the robust spline normalisation (RSN) method. Outlier samples, poor quality probes (detection threshold < 0.01) and probes that were not detected were removed from downstream analysis. R package ‘Limma’ was then used to perform a differential expression analysis with *p*-values adjusted using the Benjamini–Hochberg method [22] to take into account the false discovery rate (FDR). Analysis was performed by the Bioinformatics Support Unit (Newcastle University).

Data can be found at GSE233350.

2.7. RNA-Seq Analysis

Fastq files were downloaded from NCBI GEO (GSE211638, [23]), and RNA-STAR [24] analysis was performed to align raw reads to genome build GRCh37/hg19; QC checks were performed with FastQC. Gene counts were generated using ht-seq count [25] and Gencode v19. Differential expression analysis was carried out using the DESeq2 [26] package (R/Bioconductor) to compare the vehicle versus 10 nM DHT-treated samples.

2.8. Chromatin Immunoprecipitation Assays

LNCaP-AI and LNCaP cells were reverse-transfected with either 25 nM N/S or a pool of 2 *KMT5A*-targeting siRNAs for 72 h in steroid-depleted media followed by chromatin immunoprecipitation as described by Schmidt et al. [27].

For immunoprecipitations, 2 µg of H4K20Me1 (Ab9051, AbCam) or 2 µg of a non-specific isotype control (DAKO) was used. qPCR analysis of immunoprecipitated DNA was performed using primers specific to the *CDC20* promoter (Fwd: 5′-CCGCTAGACTCTCGTG ATAGC-3′; Rev: 5′-TGGCTCCTTCAAAATCCAAC-3′) as previously described [28]. The average fold difference of the % input between experimental arms for at least three independent experiments is presented.

2.9. Sulforhodamine B Growth Analysis

Cellular growth was assessed as described [21].

2.10. Gamma H2AX Assay

Knockdown was carried out over 72 h in LNCaP-AI and LNCaP cells using either N/S or *KMT5A*-targeting siRNA. Cells were harvested and stained for phospho-histone H2AX (Ser139) as previously described [21].

3. Results

3.1. Identification of *KMT5A*-Regulated Genes in Androgen-Independent Prostate Cancer

KMT5A has been proposed as a therapeutic target in prostate cancer; however, in this context, *KMT5A* is still largely understudied. Indeed, no study has identified which genes *KMT5A* can regulate in castration-resistant prostate cancer. To this end, *KMT5A* mRNA was knocked down using two independent siRNA sequences in the LNCaP-AI cell line model of androgen independence. After 72 h of knockdown under steroid-depleted conditions, the androgen, DHT (10 nM), was applied for 24 h prior to RNA isolation and analysis using an Illumina Human HT-12 microarray.

The significant knockdown of *KMT5A*, with both siRNAs, was confirmed within the microarray data set as >80% prior to further analysis (Figure 1A). In the presence of an active AR found after stimulation with DHT for 24 h, we found 408 genes up-regulated and 310 genes down-regulated. (Supplementary Tables S2 and S3). Of these genes, 29% have previously been shown to be AR-regulated in LNCaP cells (Supplementary Tables S2 and S3) [23]. In order to understand which cellular pathways and biological processes are affected under these conditions, the gene lists generated were used in KEGG pathway analysis and gene ontology analysis using DAVID [29,30]. We did observe a level of inconsistency between

the siRNA oligos even though the level of *KMT5A* knockdown was consistent (Figure 1A), a common issue when using siRNAs to assess multiple gene expressions, highlighting the importance of further validation studies on any target identified. Hence, all genes which showed a statistically significant change irrespective of the siRNA sequence were included in gene lists for this analysis to enhance confidence in the pathways and genes identified. This analysis revealed the significant up-regulation of PI3K-Akt signalling, apoptosis, p53 signalling and signal transduction whilst the pathways found to be significantly down-regulated included splicing, protein folding, cell division and transcriptional regulation (Supplementary Tables S4–S7). Taken together, the cellular processes and genes altered in this analysis further support our hypothesis that *KMT5A* is a potential therapeutic target for prostate cancer.

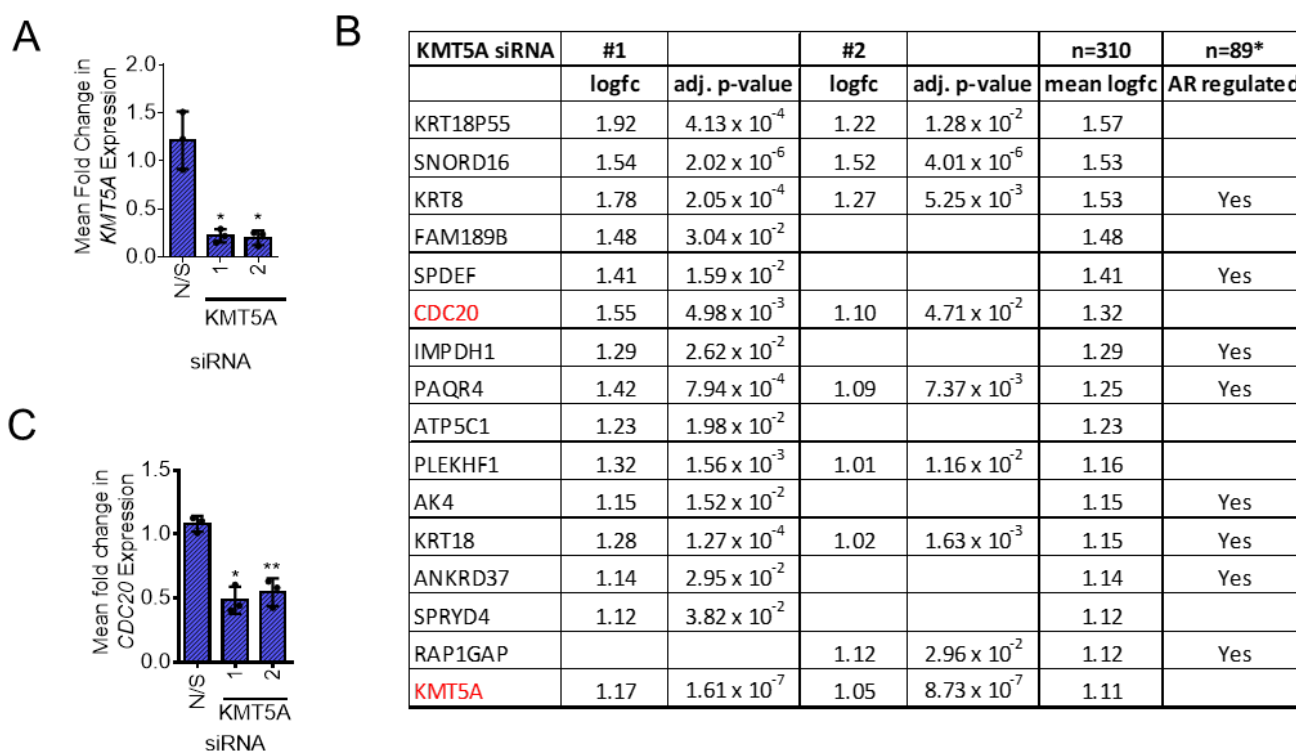


Figure 1. *KMT5A*-regulated genes in LNCaP-AI cells. (A) LNCaP-AI cells reverse-transfected with 25 nM siRNA targeting *KMT5A* or a non-silencing control (N/S) in steroid-depleted media. After 72 h, 10 nM DHT was added to the cells for a further 24 h. RNA was isolated, quality-checked, and its gene expression profiles determined using Illumina HT-12 v4.0 Expression BeadChip Microarray. Three independent experimental repeats were performed. Data analysis confirmed successful *KMT5A* knockdown. (B) Table of genes ranked for their down-regulation in response to *KMT5A* knockdown in the presence of DHT stimulation. Genes which were down-regulated more than *KMT5A* are shown (full gene lists can be found in the Supplementary Information). *GSE211638 [23]. (C) *CDC20* expression levels in response to *KMT5A* knockdown as determined via microarray analysis. One-way ANOVA with Dunnett's multiple comparisons test. * $p < 0.05$; ** $p < 0.01$.

In terms of individual genes which were down-regulated in response to *KMT5A* knock-down, *CDC20* was identified as the sixth most down-regulated gene after AR-regulated genes such as *KRT8* and *SPDEF* (Figure 1B,C). Due to its role in the cell cycle and previous characterisation as an oncogene [14,17], this gene was chosen for further study as a potential pharmacodynamic biomarker for *KMT5A* therapeutic targeting and a *KMT5A* effector protein.

3.2. KMT5A Depletion Reduces CDC20 Expression

In order to validate *CDC20* as a *KMT5A*-regulated gene, further experiments were conducted in both LNCaP-AI cells and the parental, androgen-sensitive LNCaP cell line. *KMT5A*-targeting siRNAs were transfected into both cell lines in steroid-depleted media for 72 h prior to stimulation with 10 nM DHT or the vehicle for a further 24 h. qPCR confirmed a significant reduction in the expression of *CDC20* in LNCaP-AI cells (Figure 2A) when *KMT5A* was knocked down ($p < 0.01$) (Figure 2B), which is consistent with our microarray data (Figure 1C). In addition, parental LNCaP cells also exhibited a significant reduction in *CDC20* expression (Figure 2C) irrespective of DHT stimulation upon significant *KMT5A* knockdown ($p < 0.001$) (Figure 2D). Furthermore, a robust reduction in *CDC20* protein levels was consistently observed in both cell lines (Figure 2E,F) confirming that *CDC20* is regulated by *KMT5A*, at the level of transcription, in both cell lines irrespective of AR activation.

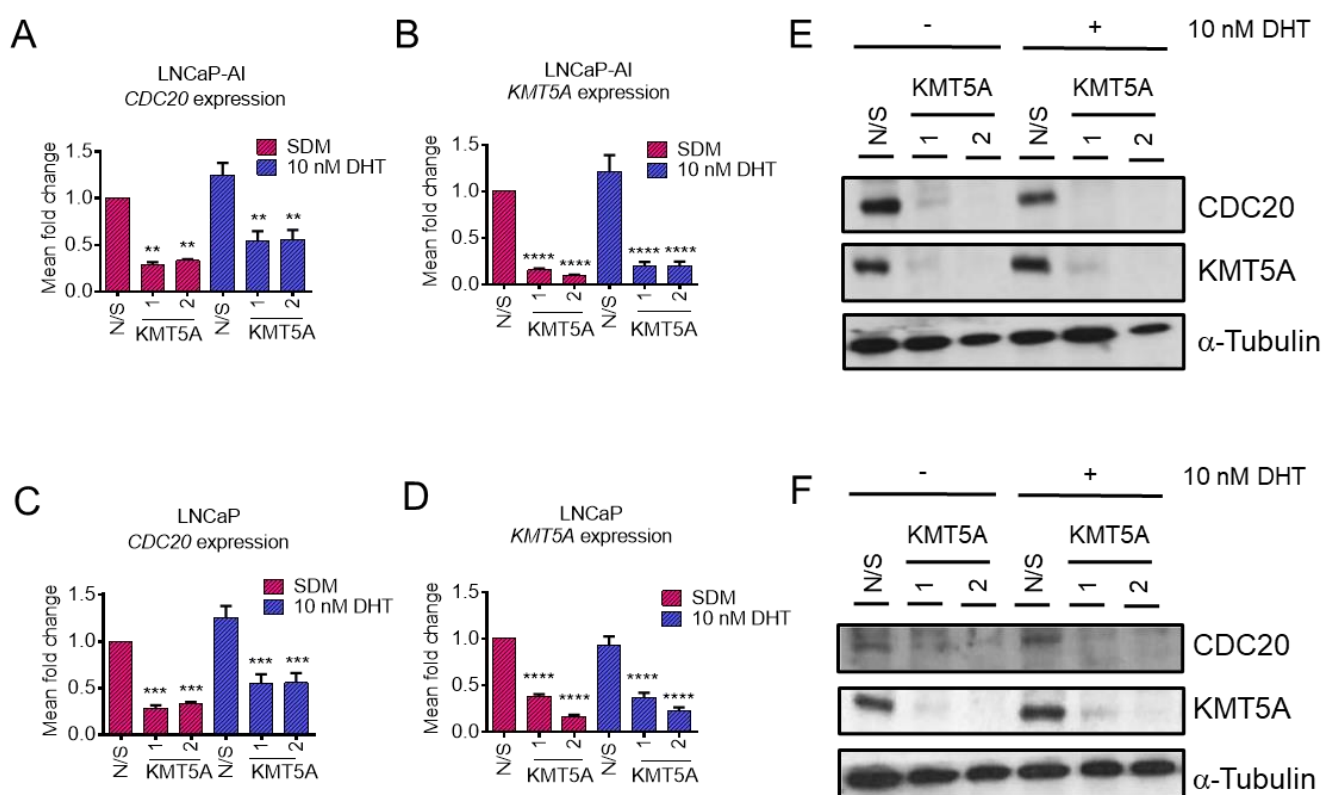


Figure 2. *CDC20* is a *KMT5A*-regulated gene. (A) LNCaP-AI cells were reverse transfected with 25 nM siRNAs targeting *KMT5A* or a non-silencing control (N/S) in steroid-depleted media. After 72 h, 10 nM DHT or a vehicle control was added to the cells for a further 24 h. RNA was isolated and *CDC20* mRNA and (B) *KMT5A* mRNA were quantified via qPCR. The same experiment was performed in (C) LNCaP cells, and *CDC20* levels and (D) *KMT5A* knockdown were confirmed via qPCR. Data are expressed as the mean fold change over 3 independent experiments, \pm SEM. (E) Determination of the protein levels of *CDC20* and *KMT5A* via Western blotting in LNCaP-AI and (F) LNCaP cells. Alpha-tubulin was used as a loading control. Data shown are representative of 3 independent experiments. Two-way ANOVA with Dunnett's multiple comparisons test; ** $p < 0.01$; *** $p < 0.001$; **** $p < 0.001$. The uncropped blots are shown in File S1.

3.3. *CDC20* Depletion Does Not Enhance *KMT5A* Protein Expression

KMT5A is phosphorylated to protect it from ubiquitin-mediated degradation by APC^{cdh1} during late mitosis [7]. In addition, due to the similarity in recognition mechanisms between CDH1 and *CDC20* for targeting proteins to the APC complex, it was suggested that *CDC20* may also bind and recognise *KMT5A* in the absence of phosphorylation [7].

This raised the question of whether or not a feedback mechanism exists between these two proteins to help maintain correct cell cycle progression. To test this theory, *CDC20* was knocked down in our cell line models and *KMT5A* levels were assessed at both the transcript and protein level. Interestingly, when *KMT5A* protein levels were examined subsequent to *CDC20* knockdown, no change was observed (Figure 3A,B), suggesting that *KMT5A* protein turnover does not take place when *CDC20* is present in the cell. However, a decrease in *KMT5A* transcripts by ~50% was observed in both cell lines (Figure 3C,D) upon the robust depletion of *CDC20* (Figure 3E,F) although this was not statistically significant. Therefore, it was concluded that *CDC20* did not play a significant role in *KMT5A* protein regulation under our experimental conditions and that *KMT5A* sits upstream of *CDC20*.

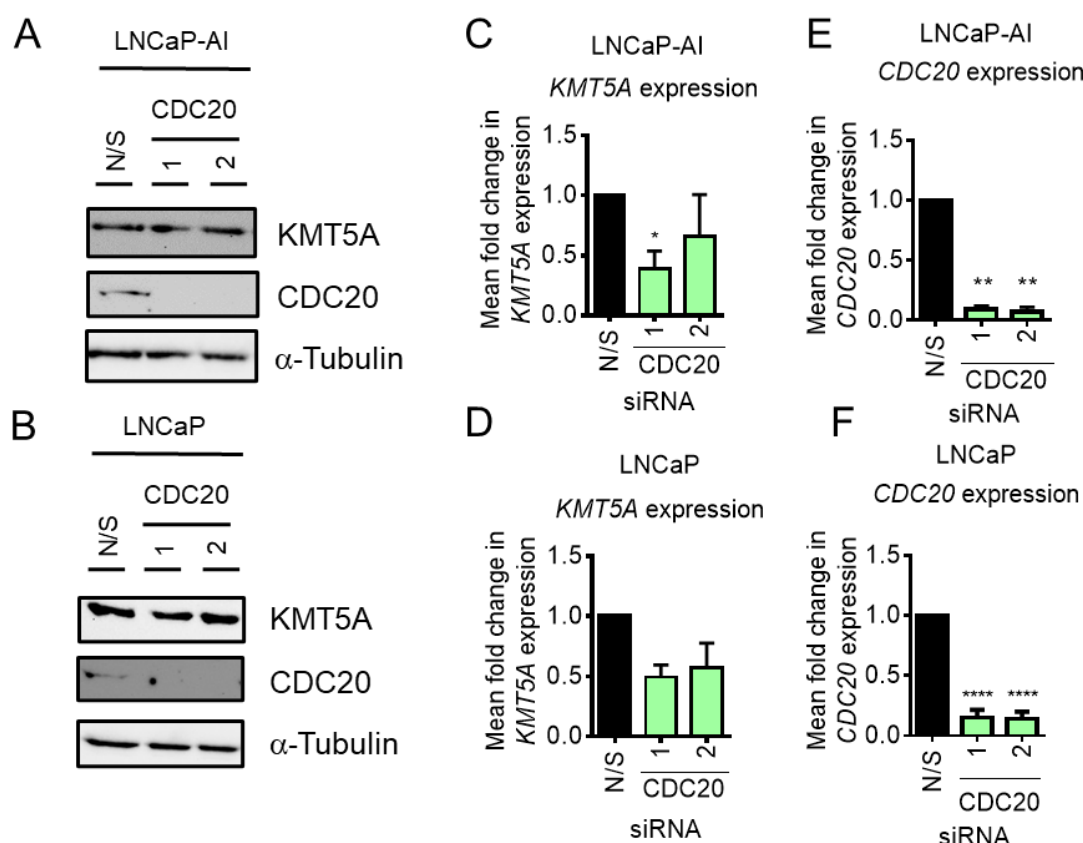


Figure 3. *CDC20* knockdown does not affect *KMT5A* protein levels. (A) LNCaP-AI cells and (B) LNCaP cells reverse-transfected with 25 nM siRNA targeting *CDC20* or a non-silencing control (N/S) for 72 h prior to analysis via Western blot analysis. Alpha-tubulin was used as a loading control. (C) LNCaP-AI and (D) LNCaP cells reverse-transfected with 25 nM siRNA targeting *CDC20* or a non-silencing control (N/S) for 72 h prior to RNA isolation and qPCR analysis for *KMT5A* and (E,F) *CDC20* mRNA levels. *HPRT1* was used as a housekeeping gene. Data are expressed as mean fold change \pm SEM. One-way ANOVA was used to determine statistical significance. * $p < 0.05$; ** $p < 0.01$; *** $p < 0.0001$. The uncropped blots are shown in File S1.

3.4. *KMT5A* Expression Correlates with *CDC20* Expression in Prostate Cancer Patients

To confirm whether or not our in vitro findings could be translated into clinical specimens of prostate cancer, we interrogated publicly available datasets to confirm a positive correlation between *CDC20* and *KMT5A* transcripts. Upon the interrogation of data sets available in cBioportal [31,32], we found a significant positive correlation between *KMT5A* and *CDC20* transcripts in a number of data sets. In a cohort of 65 treatment-naïve radical prostatectomies [33] a positive correlation between *CDC20* and *KMT5A* transcripts was observed (Spearman = 0.45; $p = 0.0002$) (Figure 4A). Similarly, in the MCTP dataset [34], a positive correlation was also observed (Spearman = 0.23; $p = 0.024$) (Figure 4B). However,

this dataset contains samples from primary (blue) and metastatic prostate cancer (red). Upon the correlation analysis of these individual sample types, it was observed that the correlation between *CDC20* and *KMT5A* was strongest in the primary prostate samples (Spearman = 0.28; $p = 0.033$; $n = 59$) and no statistically significant correlation was observed in the metastatic samples (Spearman = 0.034; $p = 0.85$; $n = 35$), although the sample numbers were lower. However, in the metastatic cohort reported by Robinson et al. [35] a statistically significant correlation was observed between *CDC20* and *KMT5A* (Spearman = 0.22; $p = 0.016$; $n = 118$) (Figure 4C). Furthermore, significant correlations were observed in bone metastases (Spearman = 0.41; $p = 0.0003$; $n = 72$) (Figure 4D) and liver metastases (Spearman = 0.408; $p = 0.011$; $n = 38$) (Figure 4E) in the samples from Abida et al. [36]. Interestingly, the highest positive correlation between *CDC20* and *KMT5A* expression was seen in prostate neuroendocrine carcinoma samples (Spearman = 0.68; $p < 0.0001$; $n = 49$) (Figure 4F) [37]. Taken together, this suggests that the positive correlation between *KMT5A* and *CDC20* observed in our cell line models is also observed in advanced prostate cancer.

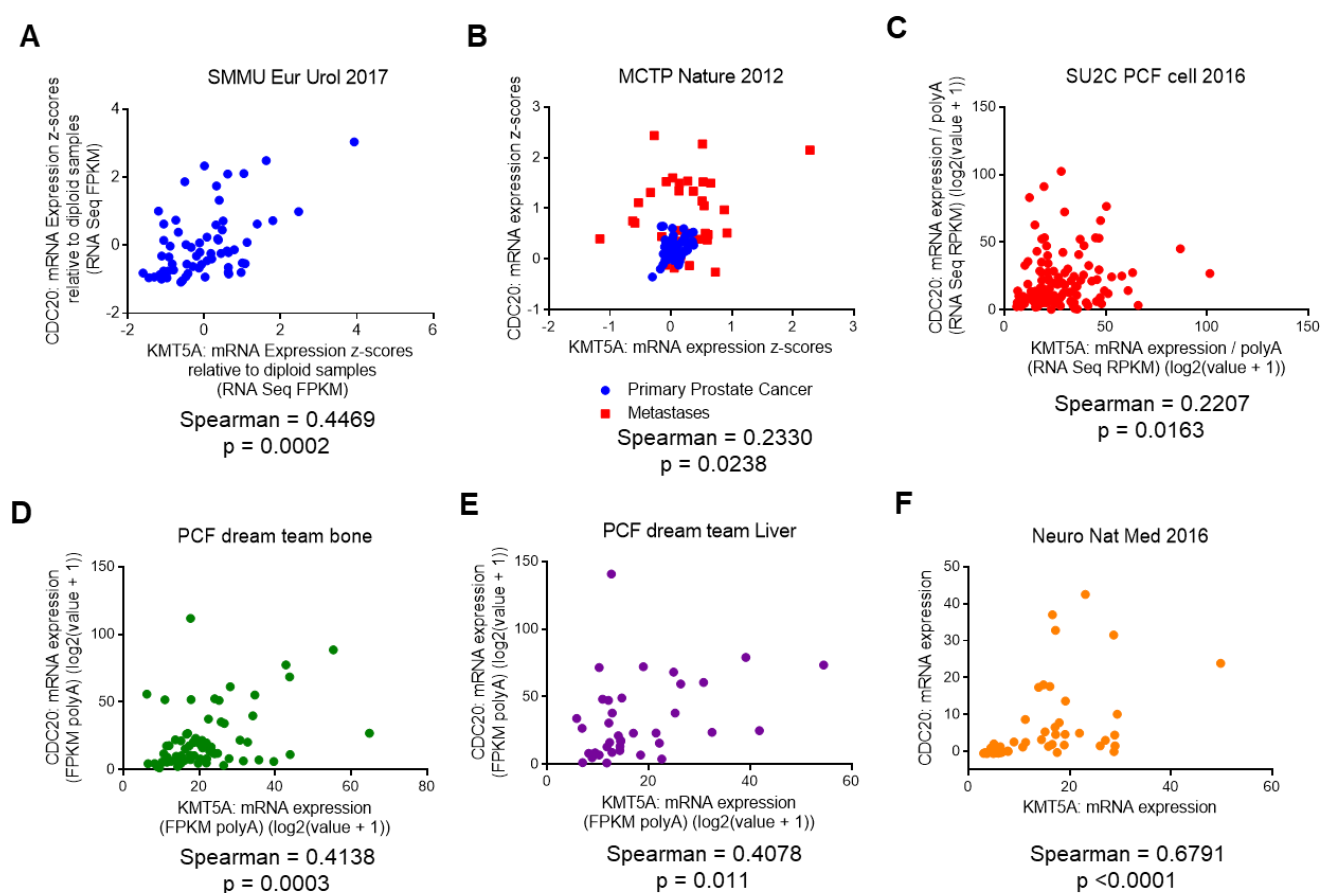


Figure 4. *KMT5A* and *CDC20* are positively correlated in clinical prostate cancer samples. Correlation in expression between *KMT5A* and *CDC20* was carried out in publicly available datasets in cBioportal. (A) Treatment naïve radical prostatectomies ($n = 65$) from [33] (B) Both primary and metastatic prostate cancer ($n = 94$) from [34] (C) Metastatic prostate adenocarcinoma samples ($n = 150$) from [35] (D) Bone metastatic prostate adenocarcinoma samples ($n = 72/266$) and (E) Liver metastatic prostate adenocarcinoma samples ($n = 38$) from [36] (F) Prostate neuroendocrine carcinoma samples ($n = 49$) from [37]. Spearman correlation (two-tailed) was calculated using Graphpad software v6.

3.5. *KMT5A* Inhibition Reduces *CDC20* Expression and Reduces Prostate Cancer Cell Proliferation

KMT5A plays a role in the cell cycle and as such, knockdown of *KMT5A* has been shown to inhibit cellular proliferation [38,39]. Indeed, we observed a reduction in proliferation upon *KMT5A* knockdown in both the cell line models used in this study

(Supplementary Figure S1A–C). In particular, proliferation was most affected under steroid depleted conditions. Furthermore, as expected, knockdown of *CDC20* resulted in a robust and significant inhibition of cellular proliferation (Supplementary Figure S1D,E). Together this provides supporting evidence that both proteins play a role in prostate cancer cell proliferation.

In order to confirm that the methyltransferase activity of KMT5A is important for the regulation of *CDC20* expression in prostate cancer cell lines we used two molecules that have shown inhibitory activity against KMT5A, namely UNC0379 and Ryuvidine [40,41] (Supplementary Figure S2). Firstly, we determined the GI50 values for LNCaP and LNCaP-AI cells (Figure 5A). Interestingly, we found that Ryuvidine was a more potent inhibitor than UNC0379 in LNCaP cells, However, in LNCaP-AI cells there was not such a large difference in efficacy. Secondly, we used a titration of doses of both inhibitors and investigated the dose dependent effects on both KMT5A and its target histone mark, H4K20Me1. We observed that UNC0379 resulted in a robust decrease in H4K20Me1 levels in LNCaP-AI and a modest reduction in LNCaP cells when total H4 levels are taken into account. This coincided with a decrease in KMT5A protein levels in LNCaP cells whilst KMT5A levels showed minimal change in LNCaP-AI cells. Ryuvidine also demonstrated a dose dependent reduction in KMT5A activity in LNCaP cells whilst a decrease in H4K20Me1 was more difficult to achieve in LNCaP-AI cells thereby reflecting the sensitivity differences to Ryuvidine between these two cell lines (Supplementary Figures S2 and S3).

Using the GI50 concentrations for each drug in LNCaP-AI cells we investigated the levels of *CDC20* by Western blotting, demonstrating that both drugs result in *CDC20* reduction (Figure 5B). Furthermore, when the more potent Ryuvidine was used in LNCaP cells at the GI50 dose a reduction in *CDC20* levels was observed (Figure 5C). Together, this led us to conclude that KMT5A enzymatic activity is important in the regulation of *CDC20* protein levels.

3.6. KMT5A Knockdown Reduces H4K20Me1 at the *CDC20* Promoter

In order to confirm that KMT5A can directly regulate the expression of *CDC20* via the mono-methylation of its only histone target, H4K20, chromatin immunoprecipitation assays were performed in both LNCaP-AI and LNCaP cells subsequent to *KMT5A* knockdown using a siRNA pool of siKMT5A_1 and siKMT5A_2. Upon *KMT5A* knockdown in both cell lines growing in steroid depleted media, a significant reduction in H4K20Me1 was observed at the *CDC20* promoter region (Figure 6A,B). This led us to conclude that KMT5A can directly modulate the expression of *CDC20* via the methylation of H4K20 within the promoter region.

3.7. p53 Mediates KMT5A Regulation of *CDC20* Expression

Whilst KMT5A methyltransferase activity is important in regulating the expression of *CDC20* via the regulation of H4K20Me1 within the *CDC20* promoter, KMT5A can also methylate non-histone proteins, including p53, to regulate functional activity. Interestingly, in our pathway analysis we uncovered some pathways within which *CDC20* can be modulated. In particular, p53 directly down-regulates *CDC20* expression via association with its promoter in response to DNA damage [11]. Secondly, in the absence of DNA damage, p53 can regulate *CDC20* expression via a CDE-CHR element, independent of p21, when p53 is over-expressed [11,14,42]. To determine whether or not DNA damage in response to KMT5A knockdown was influencing this mechanism, we investigated the levels of γ -H2AX in both LNCaP-AI and LNCaP cells after *KMT5A* knockdown. Consistent with other reports [39], *KMT5A* knockdown resulted in an increased level of DNA damage as denoted by a robust ~3.5 fold and ~2 fold increase in γ -H2AX levels in LNCaP-AI cells and LNCaP cells, respectively (Figure 7A), further suggesting that p53 could be a mediator of KMT5A effects on *CDC20* levels. Indeed, KMT5A is well-known to methylate p53 at K382 to reduce p53 activation [6], and the down-regulation of KMT5A in response to DNA damage has been shown to result in the conversion of this mono-methylation state into a di/tri- methylation

state on K382 to increase p53 stability [6,43]. Therefore, we hypothesised that knockdown of *KMT5A* would shift the equilibrium from mono-methylated p53 to acetylated p53, thereby resulting in p53 activation and the subsequent repression of *CDC20* expression. To test this theory, *KMT5A* was knocked down in both LNCaP-AI and LNCaP cells prior to Western blotting for changes in p53 post-translational modifications and MDM2. We observed no alterations in total p53 protein levels in either cell line with siKMT5A_2; however, p53 levels were increased with siKMT5A_1. Nonetheless, a robust increase in acetylation at K382 and an increase in p53-phosphorylation at serine 15 which is associated with enhanced DNA binding was still observed with both siRNA sequences (Figures 7B,C and S6). To confirm that p53 activation results in the down-regulation of *CDC20* protein levels, we treated both LNCaP-AI and LNCaP cells with the MDM2 inhibitor, Nutlin 3. In both cell lines, *CDC20* protein levels were reduced when p53 was activated (Figure 7D). Taken together, this suggests that p53 activation via *KMT5A* knockdown results in the repression of *CDC20*.

3.8. *CDC20* Is Down-Regulated by Protein Turnover in the Absence of p53

As p53 signalling was found to be up-regulated in our KEGG pathway analysis (Supplementary Table S4), we questioned whether or not *KMT5A* was able to regulate *CDC20* if p53 was not present. As p53 loss is a common phenomenon in cancers, this raised questions regarding the applicability of *CDC20* as a *KMT5A* biomarker for those patients whose tumours lack p53 expression. To investigate further, we performed *KMT5A* knockdowns in p53 null, PC3 cells and performed Western blotting and qPCR analyses of *CDC20* levels. Surprisingly, *KMT5A* knockdown was still able to robustly reduce *CDC20* protein levels in this cell line (Figure 8A). However, *CDC20* mRNA levels were unaffected (Figure 8B) suggesting that *CDC20* post-translational changes occurred causing alterations in protein turnover in the absence of p53. Therefore, if a protein biomarker read-out could be used then *CDC20* may remain as a valid *KMT5A* activity biomarker.

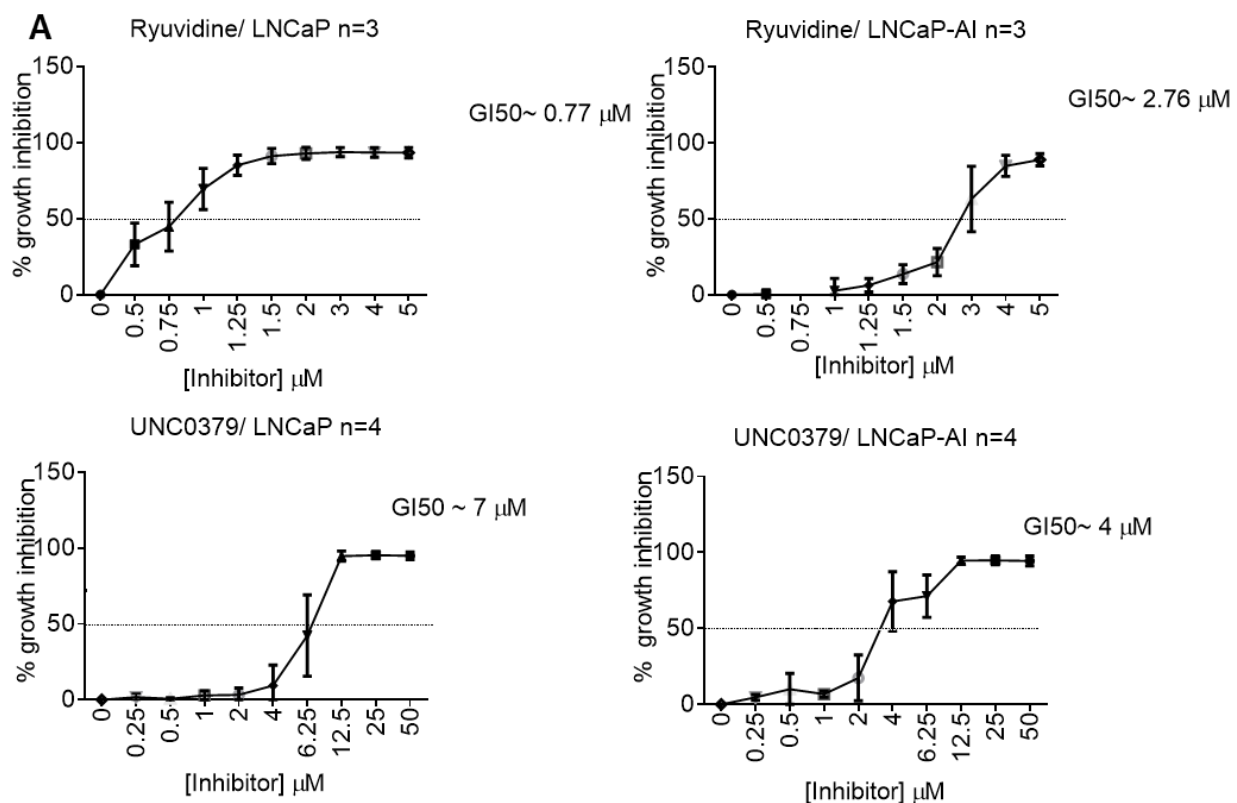


Figure 5. Cont.

Cell Line.	UNC0379 (GI50 +/- SD)	Ryuvidine (GI50 +/- SD)
LNCaP	7.06 +/- 1.88	0.77 +/- 0.19
LNCaP-AI	3.87 +/- 1.33	2.77 +/- 0.36

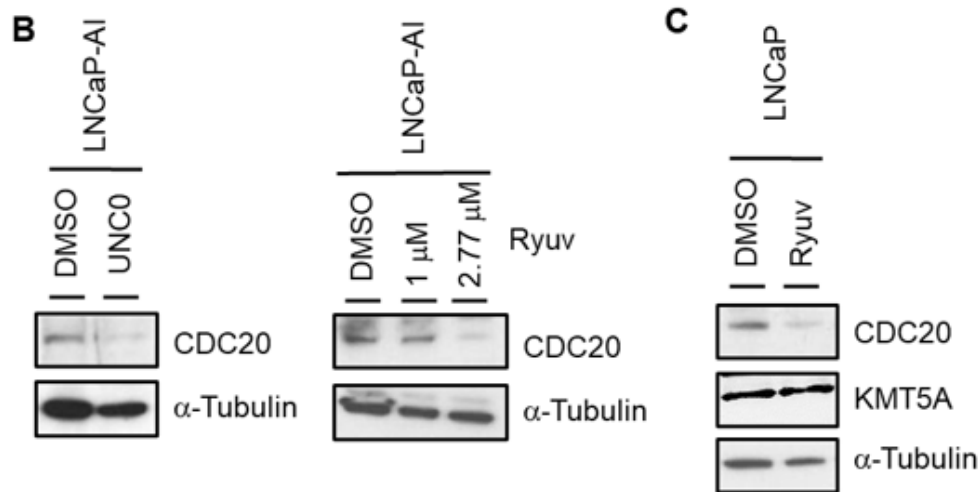


Figure 5. KMT5A inhibitors restrict prostate cancer cell growth and down-regulate CDC20. (A) LNCaP-AI and LNCaP cells treated with a dose range of UNC0379 or Ryuvidine and GI50 concentrations determined via SRB assay after 3 doubling times. Data are expressed as mean % growth inhibition \pm SEM from 3 independent experiments. Mean GI50 values are tabulated \pm SD. (B) LNCaP-AI cells treated with either UNC0379 (7 μ M) or Ryuvidine (1 μ M or 2.77 μ M) for 48 h prior to protein analysis via Western blotting. (C) LNCaP cells were treated with Ryuvidine (0.7 μ M) for 48 h prior to protein analysis via Western blotting. Data shown are representative of 3 independent experiments. The uncropped blots are shown in File S1.

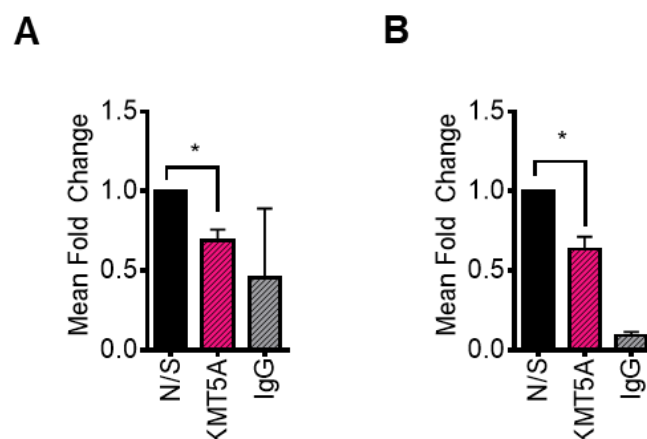


Figure 6. H4K20Me1 is reduced at the CDC20 promoter in response to KMT5A knockdown. *KMT5A* was knocked down in (A) LNCaP-AI and (B) LNCaP cells growing in steroid depleted media for 72 h. Chromatin was collected, and immunoprecipitation for H4K20Me1 carried out. Isolated DNA was purified and primers targeting the *CDC20* promoter region were used to determine the levels of H4K20Me1 association with this region. Experiments were performed 3 times and data are expressed as the mean fold change relative to the non-silencing control, \pm SEM. IgG was used as a negative control. Student's *t*-test * $p < 0.05$.

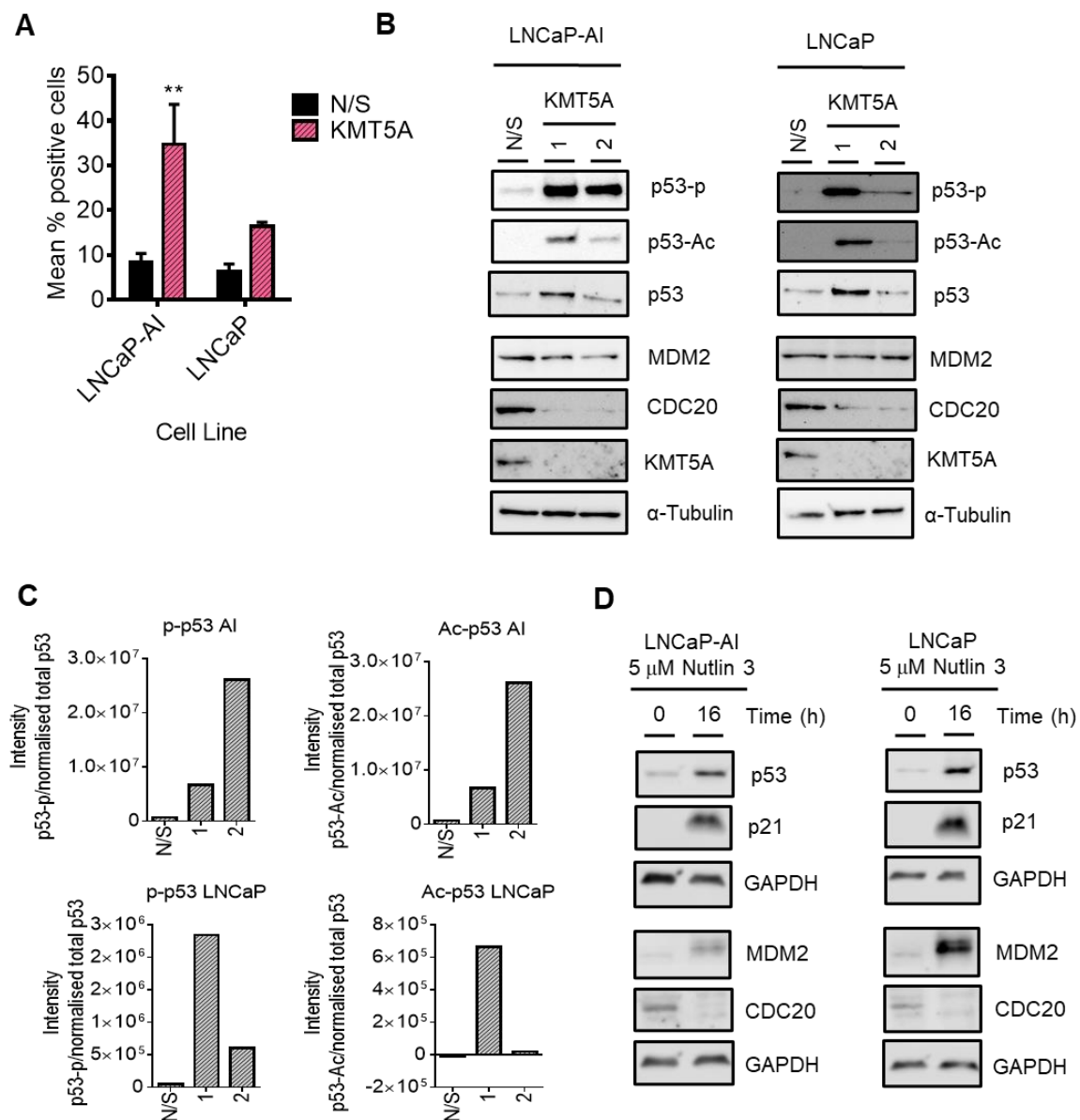


Figure 7. KMT5A regulates *CDC20* via p53 activation. **(A)** LNCaP-AI and LNCaP cells reverse transfected with either a pool of 3 *KMT5A*-targeting siRNAs or a non-silencing (N/S) control for 72 h prior to the assessment of γ -H2AX via flow cytometry. Scatter plots for experimental replicates can be found in Supplementary Figure S4. **(B)** LNCaP-AI and LNCaP cells reverse-transfected with 2 independent siRNA sequences for 72 h prior to Western blotting analysis for *CDC20*, p53, p-p53, p53-Ac, MDM2, and KMT5A. **(C)** Densitometry of Western blots shown in **(B)**. The background was subtracted from the intensity values prior to intensity normalisation against an appropriate loading control. Intensities for post-translationally modified proteins were normalised to total protein intensity. Additional experimental repeats can be found in Supplementary Figure S6. **(D)** LNCaP-AI and LNCaP cells were treated with Nutlin 3 (5 μ M) for 0 and 16 h prior to Western blotting analysis. Western blot data shown is representative of 3 independent experiments. Two-way ANOVA test was used to determine statistical significance for data shown in **(A)**. ** $p < 0.01$ The uncropped blots are shown in File S1.

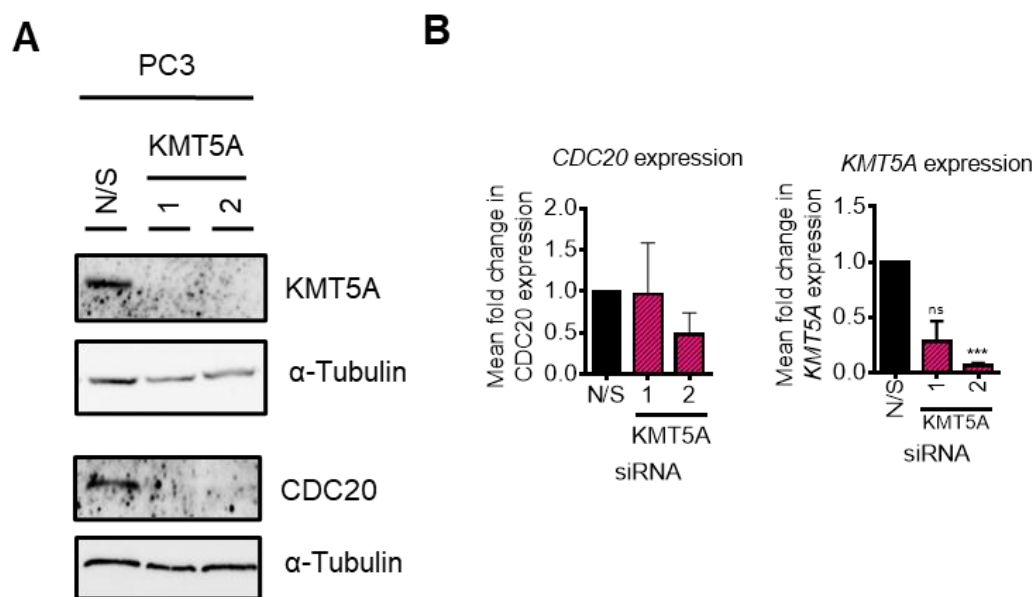


Figure 8. KMT5A regulates protein turnover in the absence of p53. (A) *KMT5A* was knocked down with 2 independent siRNAs for 72 h. Protein was collected and analysed via Western blotting for *KMT5A* and *CDC20*, and α -tubulin was used as a loading control. (B) Expression of *CDC20* and *KMT5A* in a parallel experiment analysed via qPCR. Data are shown as the mean fold change relative to that of N/S controls over 3 experimental repeats, \pm SEM. One-way ANOVA was used to determine statistical significance. *** $p < 0.01$; ns: not significant. The uncropped blots are shown in File S1.

4. Discussion

Alternative therapeutic targets are urgently required for the treatment of advanced prostate cancers which have relapsed after current standard-of-care therapies. As the androgen receptor remains a driver of disease in therapy relapse, proteins which positively modulate the transcriptional activity of the androgen receptor are proposed as putative therapeutic targets. The protein methyltransferase *KMT5A* has been shown to interact with the androgen receptor [4] and was proposed to offer therapeutic benefits to prostate cancer patients. However, the mechanisms by which *KMT5A* contributes to prostate cancer progression remains poorly understood.

We uncovered that *KMT5A* can regulate the levels of the cell cycle regulator protein *CDC20* both directly at the chromatin level via the modulation of histone methylation, and indirectly via the methylation of the tumour suppressor protein, p53. This relationship between *CDC20* and *KMT5A* is supported by a significant positive correlation between *KMT5A* and *CDC20* transcripts in prostate cancer patients (Figure 4). Whilst this relationship is independent of the androgen receptor (Figures 2 and S5), both proteins are described as oncogenes in prostate cancer. Critically, there are no reports describing the methylation-specific regulation of *CDC20*.

KMT5A is the only known methyltransferase to monomethylate histone H4K20. As the H4K20Me1 mark is traditionally associated with a compact chromatin landscape and gene repression [44–47], it is counterintuitive that *KMT5A* should function to facilitate *CDC20* transcription. However, *KMT5A*-mediated H4K20Me1 is now well-documented to function as a transcriptional activator for some genes [48,49]. Where this has been observed, there is generally a transcription factor which is implicated, for example *TWIST* [48]. Furthermore, H4K20Me1 is associated with actively transcribing gene bodies [50] and more recently has been found to result in chromatin accessibility in highly transcribed genes throughout the cell cycle [51]. A role for *KMT5A* in the pause and release of RNA pol II has also been revealed [52], further supporting the complex role of *KMT5A* in the positive regulation of gene transcription.

The methylation-dependent regulation of p53 activity by KMT5A is key to ensuring transcriptional activation [6,43], further highlighting the ability of KMT5A to influence gene expression programmes at multiple levels. Consistently, we observed that knockdown of *KMT5A* resulted in enhanced p53 acetylation at K382, which can only occur if this residue is not methylated. Importantly, it is the subsequent phosphorylation event at S15 which facilitates the association of p53 with DNA which is enhanced upon *KMT5A* knockdown. This would permit the recruitment of HDAC1 and mSin3a to the *CDC20* promoter to allow chromatin remodelling to occur and thereby inhibit the transcription of *CDC20* [11]. Importantly, we observed slightly different effects with each *KMT5A*-targeting siRNA in this experiment with regard to the ability of *KMT5A* knockdown to stabilise p53, making the interpretation of p53 post-translational modifications more complex. However, densitometry confirmed that both p53 phosphorylation and acetylation do increase with *KMT5A* knockdown with both siRNA sequences (Figure 7C). Therefore, it appears that there are two complementary mechanisms working together at the *CDC20* promoter modulated by *KMT5A* to ensure the timely expression of this gene.

Both *KMT5A* and *CDC20* are essential cell cycle regulator proteins. *KMT5A* is regulated by ubiquitin-mediated protein turnover specifically at the G1/S transition and between metaphase and anaphase [7] whilst *CDC20* regulates the SAC to control the progression from metaphase to anaphase and ensure the successful separation of sister chromatids. It is thought that the methylation of H4K20 is key to successful mitosis with the turnover of *KMT5A* being the major mode of H4K20 methylation regulation. Indeed, H4K20Me-mediated chromosome condensation is important in this process and *KMT5A* knock out studies resulted in chromosome decondensation leading to cell cycle arrest at G2/M [46]. Furthermore, H4K20Me1 is required for kinetochore assembly at centromeres via the recruitment of CENP-T [53]. Hence, it is logical to hypothesise that a lack of *KMT5A*, resulting in a decrease in H4K20Me1, will result in impaired kinetochore assembly and thereby will invoke the SAC preventing *CDC20* from facilitating the onset of the anaphase. Therefore, due to the importance of tightly regulating *CDC20* to ensure effective mitosis, the modulation of *CDC20* levels themselves by *KMT5A* would provide a failsafe way to prevent a mitotic catastrophe.

CDC20 is required for nuclear movement prior to the anaphase where its activity, as part of the APC^{CDC20} complex, results in the destruction of cyclin B and the inactivation of CDK1. Interestingly, the CDK1-mediated phosphorylation of *KMT5A* at serine 29 has been reported to occur during metaphase resulting in the removal of *KMT5A* from chromatin, holding it in a stabilised state without affecting methylase activity. It is not until anaphase that dephosphorylation by cdc14a/b permits *KMT5A* protein turnover via APC^{cdh1} [7]. Furthermore, APC^{CDC20} targets the H4K20Me1 demethylase, PHF8, for ubiquitin-mediated destruction [13] further highlighting the important relationship between *CDC20* and the enzymes which modulate the H4K20 methylation state.

CDC20 has been found to be overexpressed in a number of cancers, including prostate cancer [15,54], and there are a number of studies which demonstrate the relevance of *CDC20* to prostate cancer development and progression. For example, *CDC20* has been identified as a hub gene, alongside *CDK1*, in castration-resistant prostate cancer [55], and contributes to cell migration, disease progression and a poorer prognosis in metastatic prostate cancer [56] with another study showing that *CDC20*, alongside *PLK1* and cyclin A, plays a critical role in prostate cancer metastasis [57]. *CDC20* and *PLK1* are both located at chromosomal region 9p, which is often amplified in cancer. Indeed, high expressions of *CDC20*, *PLK1* and *CDK1* correlate with prostate cancer occurrence [58] and worse biochemical recurrence survival rates [59]. Furthermore, *CDC20* is a target protein of the Speckle-type POZ protein (SPOP), which functions to promote ubiquitin-mediated protein turnover. *SPOP* is mutated in up to 15% of prostate cancers [60] and these mutations have been shown to result in an inability of *SPOP* to associate with *CDC20*, preventing *CDC20* protein turnover and consequently resistance to *CDC20* inhibitors [16]. Both *SPOP* mutation [61] and *CDC20* overexpression are important in docetaxel resistance with the inhibition or knockdown

of *CDC20* being able to resensitise cells to docetaxel [62] highlighting the importance of *CDC20* as a therapeutic target in prostate cancer at several disease stages. With inhibitors for both *CDC20* and *KMT5A* being developed, it would be important to determine whether or not they are able to synergise with each other in drug-resistant models of prostate cancer.

KMT5A has an important role in the DNA damage repair pathway where it is recruited to double-strand breaks to deposit H4K20Me1 to facilitate Suv4-20-mediated H4K20Me2, which is required for 53BP1 binding and successful repair by NHEJ [63,64]. In addition, the ubiquitination of *KMT5A* by RNF8 increases *KMT5A* association with RNF168 which in turn promotes H2A ubiquitination [65]. The ubiquitination of these and other chromatin components results in the recruitment of BRCA1/BARD1/Abraxas and RAP80 to sites of γ H2AX to allow the repair process to take place. Interestingly, RAP80 is a target of *CDC20* and its overexpression prevents mitotic progression irrespective of DNA damage [9]. This again supports a connection between the functions of *KMT5A* and *CDC20* in cellular processes. Additionally, the role of *KMT5A* in the suppression of important anti-tumourigenic processes such as the positive regulation of the apoptotic process and the response to gamma and ionising irradiation are also highlighted suggesting the utility of *KMT5A* inhibition in combination with other DNA damage-inducing therapeutics such as radiotherapy or cytotoxic agents.

The cellular processes regulated by *KMT5A* identified in this study are consistent with those already described such as genome integrity, cell cycle progression, gene transcription and DNA damage repair. However, some novel processes were identified including RNA splicing and mRNA processing which require further investigation. This is particularly important in prostate cancer where aberrant RNA splicing, particularly of the androgen receptor, is associated with therapy resistance and poor prognosis [66].

5. Conclusions

A number of key oncogenic signalling pathways are regulated by the methyltransferase *KMT5A*. Here, we provide evidence of the role of *KMT5A* in both metaphase to anaphase control via the regulation of *CDC20* and propose that close links between mitosis and DNA damage repair processes are present via this relationship. As both *CDC20* and *KMT5A* are up-regulated in cancer via a number of mechanisms, the relationship between the two proteins may be dysregulated, thereby promoting genomic instability. This presents an opportunity to identify beneficial therapeutic combinations to treat patients based on a number of criteria such as *SPOP* mutation status, *KMT5A* expression status and therapeutic resistance.

Supplementary Materials: The following supporting information can be downloaded at <https://www.mdpi.com/article/10.3390/cancers15143597/s1>. Supplementary Figure S1. *KMT5A* and *CDC20* knockdown inhibits proliferation of prostate cancer cells. Supplementary Figure S2. *KMT5A* inhibition by UNC0379 reduces *KMT5A* levels and H4K20Me1. Supplementary Figure S3. *KMT5A* inhibition by Ryuvudine reduces *KMT5A* levels and H4K20Me1. Supplementary Figure S4. *KMT5A* knockdown causes DNA damage. Supplementary Figure S5. *KMT5A* levels remain constant in response to DHT stimulation. Supplementary Figure S6. Acetylation and phosphorylation of p53 occurs upon *KMT5A* knockdown. Table S1. qPCR primers. Table S2. Genes significantly up-regulated by *KMT5A* knockdown. Table S3. Genes significantly down-regulated by *KMT5A* knockdown. Table S4. KEGG pathways down-regulated in response to *KMT5A* knockdown in the presence of DHT stimulation. Table S5. KEGG pathways up-regulated in response to *KMT5A* knockdown in the presence of DHT stimulation. Table S6. Biological processes down-regulated in response to *KMT5A* knockdown in the presence of DHT stimulation. Table S7. Biological processes up-regulated in response to *KMT5A* knockdown in the presence of DHT stimulation. File S1. Uncut blots.

Author Contributions: Conceptualisation, K.C. and C.N.R.; Methodology, K.C. and C.N.R.; Validation, K.C., Z.A.H.A., E.L.-W. and S.N.; Formal Analysis, S.N. and Z.A.H.A.; Investigation, K.C., Z.A.H.A., M.A., D.A.-K., K.L.J., H.X.C., R.G. and S.W.; Resources, K.C. and C.N.R.; Data Curation, Z.A.H.A.; Writing—Original Draft Preparation, Z.A.H.A., M.A. and K.C.; Writing—Review and Editing, K.C., C.N.R., E.L.-W. and E.S.; Visualisation, K.C.; Supervision, K.C. and C.N.R.; Project Administration, K.C.; Funding Acquisition, K.C., Z.A.H.A. and D.A.-K. All authors have read and agreed to the published version of the manuscript.

Funding: This work was supported by a Movember funded Prostate Cancer UK Career Development Fellowship (CDF12-006) to K.C. which supported S.W., The Higher Committee for Education Development in Iraq, as a PhD studentship to Z.A.H.A., and The Public Authority of Applied Education and Training, Kuwait to D.A.-K. E.S. is supported by a Prostate Cancer UK Travelling Prize fellowship [TLD-PF19-002]. E.L.-W. is supported by a Prostate Cancer UK Research Innovation Award (RIA19-ST2-005). R.G. is supported by a William Edmond Harker Foundation Studentship. C.N.R. is supported by Cancer Research UK (C27826/A15994). For the purpose of Open Access, the author has applied a Creative Commons Attribution (CC BY) licence to any Author Accepted Manuscript (AAM) version arising from this submission.

Institutional Review Board Statement: Not applicable.

Informed Consent Statement: Not applicable.

Data Availability Statement: The microarray data presented in this study are openly available in GEO: GSE233350. Publicly available datasets were analysed in this project. This data can be found in cBioportal.

Acknowledgments: Nutlin 3 was provided as a gift from John Lunec (Newcastle Cancer Centre, Newcastle University). We thank the High-Throughput Genomics Group at the Wellcome Trust Centre for Human Genetics (funded by Wellcome Trust grant reference 090532/Z/09/Z and MRC Hub grant G0900747 91070) for the generation of the Gene Expression data. We thank Oswald To for contributions to chromatin generation for this study, Kendal Cagney for assistance with KMT5A inhibitor studies, Victoria Harle for flow cytometry assistance, and Maddie Blackham for technical assistance.

Conflicts of Interest: The authors declare no conflict of interest.

References

1. Veschi, V.; Liu, Z.; Voss, T.C.; Ozbun, L.; Gryder, B.; Yan, C.; Hu, Y.; Ma, A.; Jin, J.; Mazur, S.J.; et al. Epigenetic siRNA and Chemical Screens Identify SETD8 Inhibition as a Therapeutic Strategy for p53 Activation in High-Risk Neuroblastoma. *Cancer Cell* **2017**, *31*, 50–63. [\[CrossRef\]](#) [\[PubMed\]](#)
2. Wu, J.; Qiao, K.; Du, Y.; Zhang, X.; Cheng, H.; Peng, L.; Guo, Z. Downregulation of histone methyltransferase SET8 inhibits progression of hepatocellular carcinoma. *Sci. Rep.* **2020**, *10*, 4490. [\[CrossRef\]](#) [\[PubMed\]](#)
3. Zhang, J.; Hou, W.; Chai, M.; Zhao, H.; Jia, J.; Sun, X.; Zhao, B.; Wang, R. MicroRNA-127-3p inhibits proliferation and invasion by targeting SETD8 in human osteosarcoma cells. *Biochem. Biophys. Res. Commun.* **2016**, *469*, 1006–1011. [\[CrossRef\]](#)
4. Yao, L.; Li, Y.; Du, F.; Han, X.; Li, X.; Niu, Y.; Ren, S.; Sun, Y. Histone H4 Lys 20 methyltransferase SET8 promotes androgen receptor-mediated transcription activation in prostate cancer. *Biochem. Biophys. Res. Commun.* **2014**, *450*, 692–696. [\[CrossRef\]](#) [\[PubMed\]](#)
5. Hou, L.; Li, Q.; Yu, Y.; Li, M.; Zhang, D. SET8 induces epithelialmesenchymal transition and enhances prostate cancer cell metastasis by cooperating with ZEB1. *Mol. Med. Rep.* **2016**, *13*, 1681–1688. [\[CrossRef\]](#)
6. Shi, X.; Kachirskaa, I.; Yamaguchi, H.; West, L.E.; Wen, H.; Wang, E.W.; Dutta, S.; Appella, E.; Gozani, O. Modulation of p53 function by SET8-mediated methylation at lysine 382. *Mol. Cell* **2007**, *27*, 636–646. [\[CrossRef\]](#)
7. Wu, S.; Wang, W.; Kong, X.; Congdon, L.M.; Yokomori, K.; Kirschner, M.W.; Rice, J.C. Dynamic regulation of the PR-Set7 histone methyltransferase is required for normal cell cycle progression. *Genes Dev.* **2010**, *24*, 2531–2542. [\[CrossRef\]](#)
8. Wu, S.; Rice, J.C. A new regulator of the cell cycle: The PR-Set7 histone methyltransferase. *Cell Cycle* **2011**, *10*, 68–72. [\[CrossRef\]](#)
9. Cho, H.J.; Lee, E.H.; Han, S.H.; Chung, H.J.; Jeong, J.H.; Kwon, J.; Kim, H. Degradation of human RAP80 is cell cycle regulated by Cdc20 and Cdh1 ubiquitin ligases. *Mol. Cancer Res.* **2012**, *10*, 615–625. [\[CrossRef\]](#)
10. Chun, A.C.; Kok, K.H.; Jin, D.Y. REV7 is required for anaphase-promoting complex-dependent ubiquitination and degradation of translesion DNA polymerase REV1. *Cell Cycle* **2013**, *12*, 365–378. [\[CrossRef\]](#)
11. Banerjee, T.; Nath, S.; Roychoudhury, S. DNA damage induced p53 downregulates Cdc20 by direct binding to its promoter causing chromatin remodeling. *Nucleic Acids Res.* **2009**, *37*, 2688–2698. [\[CrossRef\]](#) [\[PubMed\]](#)

12. Kidokoro, T.; Tanikawa, C.; Furukawa, Y.; Katagiri, T.; Nakamura, Y.; Matsuda, K. CDC20, a potential cancer therapeutic target, is negatively regulated by p53. *Oncogene* **2008**, *27*, 1562–1571. [[CrossRef](#)] [[PubMed](#)]
13. Lim, H.J.; Dimova, N.V.; Tan, M.K.; Sigoillot, F.D.; King, R.W.; Shi, Y. The G2/M regulator histone demethylase PHF8 is targeted for degradation by the anaphase-promoting complex containing CDC20. *Mol. Cell Biol.* **2013**, *33*, 4166–4180. [[CrossRef](#)]
14. Wang, L.; Zhang, J.; Wan, L.; Zhou, X.; Wang, Z.; Wei, W. Targeting Cdc20 as a novel cancer therapeutic strategy. *Pharmacol. Ther.* **2015**, *151*, 141–151. [[CrossRef](#)] [[PubMed](#)]
15. Mao, Y.; Li, K.; Lu, L.; Si-Tu, J.; Lu, M.; Gao, X. Overexpression of Cdc20 in clinically localized prostate cancer: Relation to high Gleason score and biochemical recurrence after laparoscopic radical prostatectomy. *Cancer Biomark.* **2016**, *16*, 351–358. [[CrossRef](#)]
16. Wu, F.; Dai, X.; Gan, W.; Wan, L.; Li, M.; Mitsiades, N.; Wei, W.; Ding, Q.; Zhang, J. Prostate cancer-associated mutation in SPOP impairs its ability to target Cdc20 for poly-ubiquitination and degradation. *Cancer Lett.* **2017**, *385*, 207–214. [[CrossRef](#)]
17. Li, K.; Mao, Y.; Lu, L.; Hu, C.; Wang, D.; Si-Tu, J.; Lu, M.; Peng, S.; Qiu, J.; Gao, X. Silencing of CDC20 suppresses metastatic castration-resistant prostate cancer growth and enhances chemosensitivity to docetaxel. *Int. J. Oncol.* **2016**, *49*, 1679–1685. [[CrossRef](#)]
18. Li, J.; Karki, A.; Hodges, K.B.; Ahmad, N.; Zoubeydi, A.; Strebhardt, K.; Ratliff, T.L.; Konieczny, S.F.; Liu, X. Cotargeting Polo-Like Kinase 1 and the Wnt/beta-Catenin Signaling Pathway in Castration-Resistant Prostate Cancer. *Mol. Cell Biol.* **2015**, *35*, 4185–4198. [[CrossRef](#)]
19. Coffey, K.; Rogerson, L.; Ryan-Munden, C.; Alkharaif, D.; Stockley, J.; Heer, R.; Sahadevan, K.; O'Neill, D.; Jones, D.; Darby, S.; et al. The lysine demethylase, KDM4B, is a key molecule in androgen receptor signalling and turnover. *Nucleic Acids Res.* **2013**, *41*, 4433–4446. [[CrossRef](#)]
20. Bainbridge, A.; Walker, S.; Smith, J.; Patterson, K.; Dutt, A.; Ng, Y.M.; Thomas, H.D.; Wilson, L.; McCullough, B.; Jones, D.; et al. IKBKE activity enhances AR levels in advanced prostate cancer via modulation of the Hippo pathway. *Nucleic Acids Res.* **2020**, *48*, 5366–5382. [[CrossRef](#)]
21. Coffey, K.; Blackburn, T.J.; Cook, S.; Golding, B.T.; Griffin, R.J.; Hardcastle, I.R.; Hewitt, L.; Huberman, K.; McNeill, H.V.; Newell, D.R.; et al. Characterisation of a Tip60 specific inhibitor, NU9056, in prostate cancer. *PLoS ONE* **2012**, *7*, e45539. [[CrossRef](#)] [[PubMed](#)]
22. Benjamini, Y.; Hochberg, Y. Controlling the false discovery rate: A practical and powerful approach to multiple hypothesis testing. *J. R. Stat. Soc. B* **1995**, *57*, 289–300. [[CrossRef](#)]
23. Labaf, M.; Li, M.; Ting, L.; Karno, B.; Zhang, S.; Gao, S.; Patalano, S.; Macoska, J.A.; Zarringhalam, K.; Han, D.; et al. Increased AR expression in castration-resistant prostate cancer rapidly induces AR signaling reprogramming with the collaboration of EZH2. *Front. Oncol.* **2022**, *12*, 1021845. [[CrossRef](#)]
24. Dobin, A.; Davis, C.A.; Schlesinger, F.; Drenkow, J.; Zaleski, C.; Jha, S.; Batut, P.; Chaisson, M.; Gingeras, T.R. STAR: Ultrafast universal RNA-seq aligner. *Bioinformatics* **2013**, *29*, 15–21. [[CrossRef](#)] [[PubMed](#)]
25. Anders, S.; Pyl, P.T.; Huber, W. HTSeq—A Python framework to work with high-throughput sequencing data. *Bioinformatics* **2015**, *31*, 166–169. [[CrossRef](#)]
26. Love, M.I.; Huber, W.; Anders, S. Moderated estimation of fold change and dispersion for RNA-seq data with DESeq2. *Genome Biol.* **2014**, *15*, 550. [[CrossRef](#)]
27. Schmidt, D.; Wilson, M.D.; Spyrou, C.; Brown, G.D.; Hadfield, J.; Odom, D.T. ChIP-seq: Using high-throughput sequencing to discover protein-DNA interactions. *Methods* **2009**, *48*, 240–248. [[CrossRef](#)]
28. Xie, Q.; Wu, Q.; Mack, S.C.; Yang, K.; Kim, L.; Hubert, C.G.; Flavahan, W.A.; Chu, C.; Bao, S.; Rich, J.N. CDC20 maintains tumor initiating cells. *Oncotarget* **2015**, *6*, 13241–13254. [[CrossRef](#)]
29. Huang, D.W.; Sherman, B.T.; Tan, Q.; Collins, J.R.; Alvord, W.G.; Roayaei, J.; Stephens, R.; Baseler, M.W.; Lane, H.C.; Lempicki, R.A. The DAVID Gene Functional Classification Tool: A novel biological module-centric algorithm to functionally analyze large gene lists. *Genome Biol.* **2007**, *8*, R183. [[CrossRef](#)]
30. Huang, D.W.; Sherman, B.T.; Tan, Q.; Kir, J.; Liu, D.; Bryant, D.; Guo, Y.; Stephens, R.; Baseler, M.W.; Lane, H.C.; et al. DAVID Bioinformatics Resources: Expanded annotation database and novel algorithms to better extract biology from large gene lists. *Nucleic Acids Res.* **2007**, *35*, W169–W175. [[CrossRef](#)]
31. Cerami, E.; Gao, J.; Dogrusoz, U.; Gross, B.E.; Sumer, S.O.; Aksoy, B.A.; Jacobsen, A.; Byrne, C.J.; Heuer, M.L.; Larsson, E.; et al. The cBio cancer genomics portal: An open platform for exploring multidimensional cancer genomics data. *Cancer Discov.* **2012**, *2*, 401–404. [[CrossRef](#)] [[PubMed](#)]
32. Gao, J.; Aksoy, B.A.; Dogrusoz, U.; Dresdner, G.; Gross, B.; Sumer, S.O.; Sun, Y.; Jacobsen, A.; Sinha, R.; Larsson, E.; et al. Integrative analysis of complex cancer genomics and clinical profiles using the cBioPortal. *Sci. Signal* **2013**, *6*, p11. [[CrossRef](#)] [[PubMed](#)]
33. Ren, S.; Wei, G.H.; Liu, D.; Wang, L.; Hou, Y.; Zhu, S.; Peng, L.; Zhang, Q.; Cheng, Y.; Su, H.; et al. Whole-genome and Transcriptome Sequencing of Prostate Cancer Identify New Genetic Alterations Driving Disease Progression. *Eur. Urol.* **2018**, *73*, 322–339. [[CrossRef](#)] [[PubMed](#)]
34. Grasso, C.S.; Wu, Y.M.; Robinson, D.R.; Cao, X.; Dhanasekaran, S.M.; Khan, A.P.; Quist, M.J.; Jing, X.; Lonigro, R.J.; Brenner, J.C.; et al. The mutational landscape of lethal castration-resistant prostate cancer. *Nature* **2012**, *487*, 239–243. [[CrossRef](#)]
35. Robinson, D.; Van Allen, E.M.; Wu, Y.M.; Schultz, N.; Lonigro, R.J.; Mosquera, J.M.; Montgomery, B.; Taplin, M.E.; Pritchard, C.C.; Attard, G.; et al. Integrative clinical genomics of advanced prostate cancer. *Cell* **2015**, *161*, 1215–1228. [[CrossRef](#)]

36. Abida, W.; Cyrta, J.; Heller, G.; Prandi, D.; Armenia, J.; Coleman, I.; Cieslik, M.; Benelli, M.; Robinson, D.; Van Allen, E.M.; et al. Genomic correlates of clinical outcome in advanced prostate cancer. *Proc. Natl. Acad. Sci. USA* **2019**, *116*, 11428–11436. [\[CrossRef\]](#)
37. Beltran, H.; Prandi, D.; Mosquera, J.M.; Benelli, M.; Puca, L.; Cyrta, J.; Marotz, C.; Giannopoulou, E.; Chakravarthi, B.V.; Varambally, S.; et al. Divergent clonal evolution of castration-resistant neuroendocrine prostate cancer. *Nat. Med.* **2016**, *22*, 298–305. [\[CrossRef\]](#)
38. Jorgensen, S.; Elvers, I.; Trelle, M.B.; Menzel, T.; Eskildsen, M.; Jensen, O.N.; Helleday, T.; Helin, K.; Sorensen, C.S. The histone methyltransferase SET8 is required for S-phase progression. *J. Cell Biol.* **2007**, *179*, 1337–1345. [\[CrossRef\]](#) [\[PubMed\]](#)
39. Tardat, M.; Murr, R.; Herceg, Z.; Sardet, C.; Julien, E. PR-Set7-dependent lysine methylation ensures genome replication and stability through S phase. *J. Cell Biol.* **2007**, *179*, 1413–1426. [\[CrossRef\]](#)
40. Blum, G.; Ibanez, G.; Rao, X.; Shum, D.; Radu, C.; Djaballah, H.; Rice, J.C.; Luo, M. Small-molecule inhibitors of SETD8 with cellular activity. *ACS Chem. Biol.* **2014**, *9*, 2471–2478. [\[CrossRef\]](#) [\[PubMed\]](#)
41. Ma, A.; Yu, W.; Xiong, Y.; Butler, K.V.; Brown, P.J.; Jin, J. Structure-activity relationship studies of SETD8 inhibitors. *Medchemcomm* **2014**, *5*, 1892–1898. [\[CrossRef\]](#) [\[PubMed\]](#)
42. Nath, S.; Chowdhury, A.; Dey, S.; Roychoudhury, A.; Ganguly, A.; Bhattacharyya, D.; Roychoudhury, S. Deregulation of Rb-E2F1 axis causes chromosomal instability by engaging the transactivation function of Cdc20-anaphase-promoting complex/cyclosome. *Mol. Cell Biol.* **2015**, *35*, 356–369. [\[CrossRef\]](#) [\[PubMed\]](#)
43. Williams, K.; Christensen, J.; Rappsilber, J.; Nielsen, A.L.; Johansen, J.V.; Helin, K. The histone lysine demethylase JMJD3/KDM6B is recruited to p53 bound promoters and enhancer elements in a p53 dependent manner. *PLoS ONE* **2014**, *9*, e96545. [\[CrossRef\]](#) [\[PubMed\]](#)
44. Trojer, P.; Li, G.; Sims, R.J., 3rd; Vaquero, A.; Kalakonda, N.; Bocconi, P.; Lee, D.; Erdjument-Bromage, H.; Tempst, P.; Nimer, S.D.; et al. L3MBTL1, a histone-methylation-dependent chromatin lock. *Cell* **2007**, *129*, 915–928. [\[CrossRef\]](#)
45. Shoaib, M.; Walter, D.; Gillespie, P.J.; Izard, F.; Fahrenkrog, B.; Lleres, D.; Lerdrup, M.; Johansen, J.V.; Hansen, K.; Julien, E.; et al. Histone H4K20 methylation mediated chromatin compaction threshold ensures genome integrity by limiting DNA replication licensing. *Nat. Commun.* **2018**, *9*, 3704. [\[CrossRef\]](#)
46. Oda, H.; Hubner, M.R.; Beck, D.B.; Vermeulen, M.; Hurwitz, J.; Spector, D.L.; Reinberg, D. Regulation of the histone H4 monomethylase PR-Set7 by CRL4(Cdt2)-mediated PCNA-dependent degradation during DNA damage. *Mol. Cell* **2010**, *40*, 364–376. [\[CrossRef\]](#)
47. Nishioka, K.; Rice, J.C.; Sarma, K.; Erdjument-Bromage, H.; Werner, J.; Wang, Y.; Chuikov, S.; Valenzuela, P.; Tempst, P.; Steward, R.; et al. PR-Set7 is a nucleosome-specific methyltransferase that modifies lysine 20 of histone H4 and is associated with silent chromatin. *Mol. Cell* **2002**, *9*, 1201–1213. [\[CrossRef\]](#)
48. Yang, F.; Sun, L.; Li, Q.; Han, X.; Lei, L.; Zhang, H.; Shang, Y. SET8 promotes epithelial-mesenchymal transition and confers TWIST dual transcriptional activities. *EMBO J.* **2012**, *31*, 110–123. [\[CrossRef\]](#)
49. Li, Z.; Nie, F.; Wang, S.; Li, L. Histone H4 Lys 20 monomethylation by histone methylase SET8 mediates Wnt target gene activation. *Proc. Natl. Acad. Sci. USA* **2011**, *108*, 3116–3123. [\[CrossRef\]](#)
50. Vakoc, C.R.; Sachdeva, M.M.; Wang, H.; Blobel, G.A. Profile of histone lysine methylation across transcribed mammalian chromatin. *Mol. Cell Biol.* **2006**, *26*, 9185–9195. [\[CrossRef\]](#)
51. Shoaib, M.; Chen, Q.; Shi, X.; Nair, N.; Prasanna, C.; Yang, R.; Walter, D.; Frederiksen, K.S.; Einarsson, H.; Svensson, J.P.; et al. Histone H4 lysine 20 mono-methylation directly facilitates chromatin openness and promotes transcription of housekeeping genes. *Nat. Commun.* **2021**, *12*, 4800. [\[CrossRef\]](#) [\[PubMed\]](#)
52. Kapoor-Vazirani, P.; Vertino, P.M. A dual role for the histone methyltransferase PR-SET7/SETD8 and histone H4 lysine 20 monomethylation in the local regulation of RNA polymerase II pausing. *J. Biol. Chem.* **2014**, *289*, 7425–7437. [\[CrossRef\]](#) [\[PubMed\]](#)
53. Hori, T.; Shang, W.H.; Toyoda, A.; Misu, S.; Monma, N.; Ikeo, K.; Molina, O.; Vargiu, G.; Fujiyama, A.; Kimura, H.; et al. Histone H4 Lys 20 monomethylation of the CENP-A nucleosome is essential for kinetochore assembly. *Dev. Cell* **2014**, *29*, 740–749. [\[CrossRef\]](#) [\[PubMed\]](#)
54. Wu, F.; Sun, Y.; Chen, J.; Li, H.; Yao, K.; Liu, Y.; Liu, Q.; Lu, J. The Oncogenic Role of APC/C Activator Protein Cdc20 by an Integrated Pan-Cancer Analysis in Human Tumors. *Front. Oncol.* **2021**, *11*, 721797. [\[CrossRef\]](#)
55. Liang, X.; Hu, K.; Li, D.; Wang, Y.; Liu, M.; Wang, X.; Zhu, W.; Wang, X.; Yang, Z.; Lu, J. Identification of Core Genes and Potential Drugs for Castration-Resistant Prostate Cancer Based on Bioinformatics Analysis. *DNA Cell Biol.* **2020**, *39*, 836–847. [\[CrossRef\]](#)
56. Dai, L.; Song, Z.X.; Wei, D.P.; Zhang, J.D.; Liang, J.Q.; Wang, B.B.; Ma, W.T.; Li, L.Y.; Dang, Y.L.; Zhao, L.; et al. CDC20 and PTTG1 are Important Biomarkers and Potential Therapeutic Targets for Metastatic Prostate Cancer. *Adv. Ther.* **2021**, *38*, 2973–2989. [\[CrossRef\]](#)
57. Gu, P.; Yang, D.; Zhu, J.; Zhang, M.; He, X. Bioinformatics analysis identified hub genes in prostate cancer tumorigenesis and metastasis. *Math. Biosci. Eng.* **2021**, *18*, 3180–3196. [\[CrossRef\]](#)
58. Wei, J.; Yin, Y.; Deng, Q.; Zhou, J.; Wang, Y.; Yin, G.; Yang, J.; Tang, Y. Integrative Analysis of MicroRNA and Gene Interactions for Revealing Candidate Signatures in Prostate Cancer. *Front. Genet.* **2020**, *11*, 176. [\[CrossRef\]](#)
59. Luo, C.; Chen, J.; Chen, L. Exploration of gene expression profiles and immune microenvironment between high and low tumor mutation burden groups in prostate cancer. *Int. Immunopharmacol.* **2020**, *86*, 106709. [\[CrossRef\]](#)

60. Barbieri, C.E.; Baca, S.C.; Lawrence, M.S.; Demichelis, F.; Blattner, M.; Theurillat, J.P.; White, T.A.; Stojanov, P.; Van Allen, E.; Stransky, N.; et al. Exome sequencing identifies recurrent SPOP, FOXA1 and MED12 mutations in prostate cancer. *Nat. Genet.* **2012**, *44*, 685–689. [[CrossRef](#)]
61. Shi, Q.; Zhu, Y.; Ma, J.; Chang, K.; Ding, D.; Bai, Y.; Gao, K.; Zhang, P.; Mo, R.; Feng, K.; et al. Prostate Cancer-associated SPOP mutations enhance cancer cell survival and docetaxel resistance by upregulating Caprin1-dependent stress granule assembly. *Mol. Cancer* **2019**, *18*, 170. [[CrossRef](#)] [[PubMed](#)]
62. Wu, F.; Lin, Y.; Cui, P.; Li, H.; Zhang, L.; Sun, Z.; Huang, S.; Li, S.; Huang, S.; Zhao, Q.; et al. Cdc20/p55 mediates the resistance to docetaxel in castration-resistant prostate cancer in a Bim-dependent manner. *Cancer Chemother. Pharmacol.* **2018**, *81*, 999–1006. [[CrossRef](#)] [[PubMed](#)]
63. Tuzon, C.T.; Spektor, T.; Kong, X.; Congdon, L.M.; Wu, S.; Schotta, G.; Yokomori, K.; Rice, J.C. Concerted activities of distinct H4K20 methyltransferases at DNA double-strand breaks regulate 53BP1 nucleation and NHEJ-directed repair. *Cell Rep.* **2014**, *8*, 430–438. [[CrossRef](#)]
64. Dulev, S.; Tkach, J.; Lin, S.; Batada, N.N. SET8 methyltransferase activity during the DNA double-strand break response is required for recruitment of 53BP1. *EMBO Rep.* **2014**, *15*, 1163–1174. [[CrossRef](#)]
65. Lu, X.; Xu, M.; Zhu, Q.; Zhang, J.; Liu, G.; Bao, Y.; Gu, L.; Tian, Y.; Wen, H.; Zhu, W.G. RNF8-ubiquitinated KMT5A is required for RNF168-induced H2A ubiquitination in response to DNA damage. *FASEB J.* **2021**, *35*, e21326. [[CrossRef](#)]
66. Jimenez-Vacas, J.M.; Herrero-Aguayo, V.; Montero-Hidalgo, A.J.; Gomez-Gomez, E.; Fuentes-Fayos, A.C.; Leon-Gonzalez, A.J.; Saez-Martinez, P.; Alors-Perez, E.; Pedraza-Arevalo, S.; Gonzalez-Serrano, T.; et al. Dysregulation of the splicing machinery is directly associated to aggressiveness of prostate cancer. *EBioMedicine* **2020**, *51*, 102547. [[CrossRef](#)] [[PubMed](#)]

Disclaimer/Publisher's Note: The statements, opinions and data contained in all publications are solely those of the individual author(s) and contributor(s) and not of MDPI and/or the editor(s). MDPI and/or the editor(s) disclaim responsibility for any injury to people or property resulting from any ideas, methods, instructions or products referred to in the content.